The temperature dependence of the lattice parameters of pure BCC Zr and BCC Zr-2 at.%Co

1992 J. Phys.: Condens. Matter 4 727

(http://iopscience.iop.org/0953-8984/4/3/012)

J. Phys.: Condens. Matter 4 (1992) 727–733. Printed in the UK

The temperature dependence of the lattice parameters of pure BCC Zr and BCC Zr–2 at.%Co

A Heiming†, W Petry†, J Trampenau‡, W Miekeley§ and J Cockcroft†

† Institut Laue–Langevin, 156X, 38042 Grenoble Cédex, France

‡ Institut für Metallforschung, Universität Münster, 4400 Münster, Federal Republic of Germany

§ Hahn-Meitner Institut, 1000 Berlin 39, Federal Republic of Germany

Received 5 September 1991

Abstract. The temperature dependence of the lattice parameters in the β-phase (BCC structure) of pure Zr and Zr–2 at.%Co was determined between 900 and 1550 °C by neutron diffraction. All diffraction patterns show a high diffuse background, which is identified as thermal diffuse scattering and originates from particular low-energy phonons in BCC Zr and its alloys. The lattice parameter of pure BCC Zr is given by $a_{Zr} = 3.14(17)\times10^{-5}T+3.579(5)$ in Å (T in K). Alloying with Co results in a contraction of BCC Zr, from which it is concluded that Co is dissolved substitutionally. The consequences of these results for the fast diffusion of Co in BCC Zr are discussed.

1. Introduction

Metallic solutes such as Fe, Co and Ni diffuse anomalously fast in the high temperature BCC β-phase of the group IV metals Ti, Zr and Hf, i.e. diffusivities are observed, which are at least two orders of magnitude higher than the corresponding self-diffusion. Neither macroscopic investigations of the net transport of mass, using the radio-tracer technique, nor microscopic studies, using quasi-elastic neutron scattering or quasi-elastic Mössbauer spectroscopy were able to reveal, unambiguously, the underlying atomic jump mechanism [1–4].

It is the lack of information about the solute site and the solute induced lattice distortions which have, up until now, restricted the discussion of models for the atomic jump mechanism. Here we report on measurements of the bulk equilibrium lattice parameters of pure BCC Zr and Zr–2 at.%Co between 900 and 1550 °C in order to deduce the solute site of fast diffusing Co in BCC Zr. This investigation is part of an extensive study of the host–impurity interaction, using elastic and inelastic neutron scattering techniques [5–8]. Co was chosen as the solute, because microscopic measurements refer directly to this system [2]. The measurements on pure BCC Zr were taken for comparison, because the lattice parameter of pure Zr in its β-phase (BCC structure) has only been reported at 980 °C ($a_{Zr} = 3.6163(20)$ Å [9]). Within this early work corrections had to be applied in order to account for the large Hf content in the sample. Further corrections were made to take the continuous absorption of oxygen during the high temperature measurements into account.

0953-8984/92/030727+07$03.50

2. Experimental details

For the sample preparation, iodine grade Zr was obtained from Wah Chang, Albany, USA. The main impurities were (in wt ppm): Al, < 20; B, 0.25; C, < 30; Cd, < 0.25; Co, < 10; Cr, < 50; Cu, < 10; Fe, 150; H, 8; Hf, 53; Mn, < 25; Mo, < 10; N, < 5; Nb, < 50; Ni, < 35; O, < 100; P, 4; Pb, < 25; Si, 25; Sn, < 10; Ta, < 50; Ti, < 25; U, < 1; V, < 25; W, < 25. Additional analysis of the oxygen and nitrogen content by the Bundesanstalt für Materialforschung und -prüfung (BAM) in Berlin yielded 31(3) and 4(1) wt ppm, respectively. The spec-pure Co for the alloy preparation originated from Johnson Matthey, England (metallic impurities in wt ppm: Ag, < 1; Al, < 1; Ca, < 1; Cr, < 1; Cu, < 1; Fe, 2; Mg, < 1; Si, 7).

Pellets of the samples were prepared by levitation melting in a high-purity Ar atmosphere. Remelting of the pellets up to 10 times resulted in good homogeneity for the alloy. The microprobe analysis of the solute concentration yielded 2.14(20) at.%Co in the alloy. For reasons of comparison, the same melting procedure was also applied to the Zr sample.

The first diffraction measurements at 1000 °C showed that the pellets recrystallize immediately at high temperature. They were thus not ideally suitable for a powder diffraction experiment, because a preferred orientation of the grains occurred. An attempt to produce a fine powder of Zr and its alloys by ball-milling failed due to a high absorption of oxygen during the milling process. In order to obtain a sample as similar as possible to a powder, the pellets were chipped to pieces of about 5 mm length and 1 mm × 1 mm on a lathe. Surface contaminations, which occurred during the sample preparation, were carefully removed by chemical etching in a mixture of 60% H_2O, 30% HNO_3, 10% HF.

For all experiments the samples were vacuum sealed into Nb containers of 0.5 mm wall thickness to minimize the accumulation of oxygen during the high temperature measurements. In addition, the containers prevented the evaporation of Co from the sample. Despite these precautions, taken to ensure the purity of the samples, further absorption of oxygen and nitrogen turned out to be unavoidable. An analysis performed by the BAM after the measurements gave 207(15)/12(3) wt ppm in the oxygen/nitrogen content for the massive pure Zr pellets and 230(23)/27(6) wt ppm for the chipped alloyed samples, respectively.

All measurements were taken on the high-flux high-resolution neutron diffractometer D2B of the Institut Laue–Langevin in Grenoble, using an incident wavelength of $\lambda = 1.59$ Å. High temperatures were obtained using a standard vacuum furnace, with a Nb heating resistor, in which the sample was rotated continuously, around the axis perpendicular to the scattering plane, in order to improve the powder averaging.

3. Results

Measurements were performed over the whole range of existence of the BCC structure of Zr and Zr–2 at.% Co. Figure 1(*a*) shows a typical diffraction pattern of BCC Zr at 1300 °C. Quite remarkable is the high background, which is strongly modulated and shows peaks underneath the Bragg reflexions of the sample, but not underneath the Bragg peaks originating from the Nb container. This background is due to thermal diffuse scattering (TDS) and was observed for both the pure and the alloyed samples. Before discussing the results on the measurements of the lattice parameters, some calculations of the TDS are presented.

3.1. Thermal diffuse scattering

Insight into the TDS is obtained by considering the scattering intensity of neutrons or x-rays resulting from the interaction with single phonons. In the high temperature limit ($k_B T \gg \hbar\omega$, where k_B is the Boltzmann constant, T temperature and $\hbar\omega$ the phonon energy) the one-phonon structure factor for a monoatomic lattice reads [10, 11]

$$|F_j(Q)|^2 \sim b^2 \frac{|Q\sigma_j|^2}{(\hbar\omega_j)^2} e^{-2W}$$

$j = 1, \ldots, 3N$, where N is the number of atoms in the unit cell. $Q = q \pm \tau_{hkl}$ is the scattering vector and q the wavevector of the jth phonon with a displacement vector $\sigma_j(q)$ and the energy $\hbar\omega_j(q)$. τ_{hkl} is a reciprocal lattice point, b the coherent scattering length of the atoms and $\exp(-2W)$ the Debye–Waller factor.

In a standard Born–von Kármán approach, lattice vibrations are parameterized by interatomic force constants, which are obtained by a fit to the measured phonon dispersion. Using the force constants up to the fifth nearest-neighbour shell for BCC Zr [8], the phonon energy $\hbar\omega_j(q)$ and the displacement vector $\sigma_j(q)$ for any arbitrary wavevector q is easily calculated by diagonalizing the dynamical matrix. In order to calculate the scattering intensity, I, expected in an experiment without any energy analysis of the scattering events, the corresponding structure factors of the three independent phonon branches have to be added, i.e. $I \simeq \sum_{j=1}^{3} |F_j|^2$. For simulating scattering in a powder the direction of Q is chosen randomly. Its length is given by $Q^2 = k_i^2 + k_f^2 - 2|k_i||k_f|\cos(2\vartheta)$ where 2ϑ is the angle between the incident and scattered wavevectors k_i and k_f, respectively.

Results of such calculations are shown in figure 1(*b*). These calculations include the geometrical factor $1/\sin(2\vartheta)$, which accounts for the varying Debye–Scherrer cone sizes for different scattering angles 2ϑ. Two observations can be made: (1) diffuse peaks are found as satellites around the Bragg reflexions; and (2) strong intensities are calculated in between the scattering angles of the Bragg peaks.

The first observation is caused by a general property of lattice vibrations. All acoustic phonon branches approach zero, when the wavevector q reaches a reciprocal lattice point. The $(\hbar\omega)^{-2}$ dependence of the TDS intensity on the phonon energy leads to singularities in the calculations. The relative intensity of the TDS around the different Bragg peaks corresponds to the multiplicities of the reflexions. The same calculations were also performed for Nb, which was used as the container material in the experiment and resulted in Bragg reflexions in the spectra (see figure 1(*a*)). The interatomic force constants for Nb were taken from [12]. Possible temperature-dependent changes in the phonon dispersion were not included in the calculation. These simulations yield TDS intensities considerably lower than for pure BCC Zr. This is caused by the steeper initial slope of the phonon branches and the overall higher phonon energies in Nb.

The second observation of strong intensities in between the Bragg peaks originates from extremely low and damped phonons in the BCC phase of the group IV metals Ti, Zr and Hf [8, 13]. These low phonon modes contribute strongly to the TDS background and also lead to intensities away from the Bragg peaks. In this respect, the group IV metals differ from other metals such as Nb, in which no low energy phonon branches are found, and thus the calculated TDS intensity is low in between the Bragg peak in agreement with the experiment.

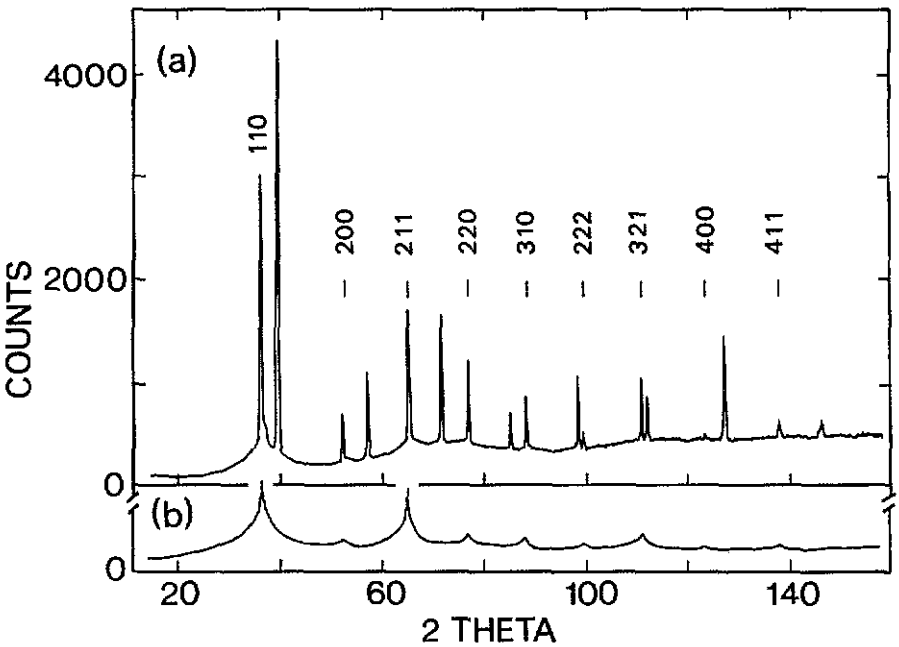

Figure 1. (*a*) Diffraction pattern of BCC Zr (chipped sample, incident wavelength $\lambda = 1.59$ Å) at 1300 °C. Note the high TDS background. The unmarked peaks originate from the Nb sample container. (*b*) Calculated TDS according to the one-phonon structure factor and the lattice vibrational spectrum of BCC Zr [8].

At high scattering angles multi-phonon processes become important, which were not considered in this simple simulation. Tentatively they can explain the disagreement between calculations and the experimentally observed background at large scattering angle, because they lead to a smooth background modulation underneath the one phonon scattering intensity (see [14]).

In contrast to x-ray investigations, the TDS can be separated from the elastic scattering in a neutron experiment by performing an energy analysis of the scattered neutrons. However, in the β-phase (BCC structure) of the group IV metals and their alloys phonon intensities would still remain in the elastic scattering intensity. They have their origin in the short lifetime (or strong damping) of the low energy phonons, which causes the observation of intensity of inelastic origin at zero energy transfer. Experimentally, this physical property of the group IV metals means that inelastic intensity is always observed, independently of how good an energy resolution is chosen (see, for example, figures 4 or 7 in [8]).

3.2. Lattice parameters

Figure 2 shows the lattice parameters of BCC Zr and BCC Zr–2 at.%Co, as obtained from a simultaneous fit of all peak positions to Bragg's law for a given temperature and sample. The temperature dependence is described in a linear approximation by

$$a_{\mathrm{Zr}} = 3.14(17) \times 10^{-5} T + 3.579(5) \text{ in Å}$$

$$a_{\mathrm{Zr-2\ at.\%Co}} = 4.45(20) \times 10^{-5} T + 3.547(3) \text{ in Å}$$

where T is given in Kelvin. Within the present study the earlier determination of the lattice parameter of BCC Zr [9] at 980 °C is confirmed. Furthermore, the temperature dependence of the lattice parameter of Nb was extracted from reflexions originating from the sample container ($a_{Nb} = 3.01(11) \times 10^{-5}T + 3.287(2)$ in Å). This result is in agreement with earlier measurements [15] in the investigated temperature range.

On lowering the temperature to go from the BCC (β-phase) to the HCP (α-phase) an expansion of the Zr lattice occurs: At $T_{\alpha\beta} = 862$ °C a lattice parameter of $a_{BCC} = 3.615$ Å is obtained from the previously noted temperature dependence. Using the crystallographic relationship between BCC and HCP, first derived by Burgers [16] (see also [6]) $a_{HCP} = \sqrt{3}/2 a_{BCC}$ and $c_{HCP} = \sqrt{2} a_{BCC}$ are obtained. This corresponds to the ideal c/a ratio for the HCP structure. Measurements on the lattice parameters of HCP Zr just below $T_{\alpha\beta}$ at 852 °C yielded [17] $a_{HCP} = 3.247$ Å and $c_{HCP} = 5.197$ Å. This result is slightly larger than expected from the geometrical relationship. Thus, on lowering the temperature, an expansion of 3.7% is found in the basal plane and of 1.6% in the c-direction. This is in agreement with the earlier observation which reported an expansion of the α-phase unit cell volume at $T_{\alpha\beta}$ [9].

Alloying Co to Zr causes a contraction of the BCC lattice. The magnitude of this contraction can be expressed as the difference between the lattice parameters of the pure and alloyed sample $\Delta a = a_{Zr} - a_{Zr-2\ at.\%Co}$, normalized to the solute concentration c and the lattice parameter of the pure sample a_{Zr}, i.e. $(\Delta a/a)c = 0.17$ is found at 1000 °C.

The observed lattice contraction of BCC Zr due to alloying with Co can be understood by a substitutional dissolution of the solutes. The atomic radius of Co is considerably smaller (about 20%) than that of a Zr atom [18]. Within this hard sphere model a substitutional solute site of the Co will yield a lattice contraction, whereas—independent of the atomic size of the solute in respect of the solvent—an interstitial site is supposed to result in an expansion, as is the case for all gaseous solutes in metals.

It is thus concluded, that the contraction of the Zr matrix due to alloying is a strong argument in favour of substitutional dissolved Co in the BCC Zr lattice.

Further evidence for this solute site was obtained by recent measurements of the Co induced lattice distortions in BCC Zr by studying the elastic diffuse scattering intensity in Zr–1.5 at.%Co single crystals [7]. It turns out, that the observed modulation of the diffuse scattering intensity can be explained fully by Co dissolved on substitutional sites, causing a radial symmetric displacement field of the matrix atoms. The absolute value of the lattice contraction $(\Delta a/a)c$ reported here was used in this explanation to describe the observed scattering intensities on an absolute scale.

Applying Vegard's law for the lattice parameters of alloys, consistency within our explanation of a substitutional dissolution of Co in BCC Zr can be verified. Accordingly, the lattice parameter of a substitutional alloy is the sum of the concentration weighted lattice parameters of the constituents. In the present case a direct comparison with this rule is not possible, because the structure of Co is HCP at room temperature ($a_{HCP} = 2.51$ Å and $c_{HCP} = 4.07$ Å [19]). However, using the previously discussed relationship between the lattice parameters of HCP and BCC Co

$$a_{Zr-2\ at.\%Co} = 0.98 \times 3.62 + 0.02 \times \frac{2}{\sqrt{3}} \times 2.51 = 3.60 \text{ Å} \qquad \text{at } 1000\,^{\circ}\text{C}$$

is obtained. This value agrees perfectly with the experimentally observed value (figure 2).

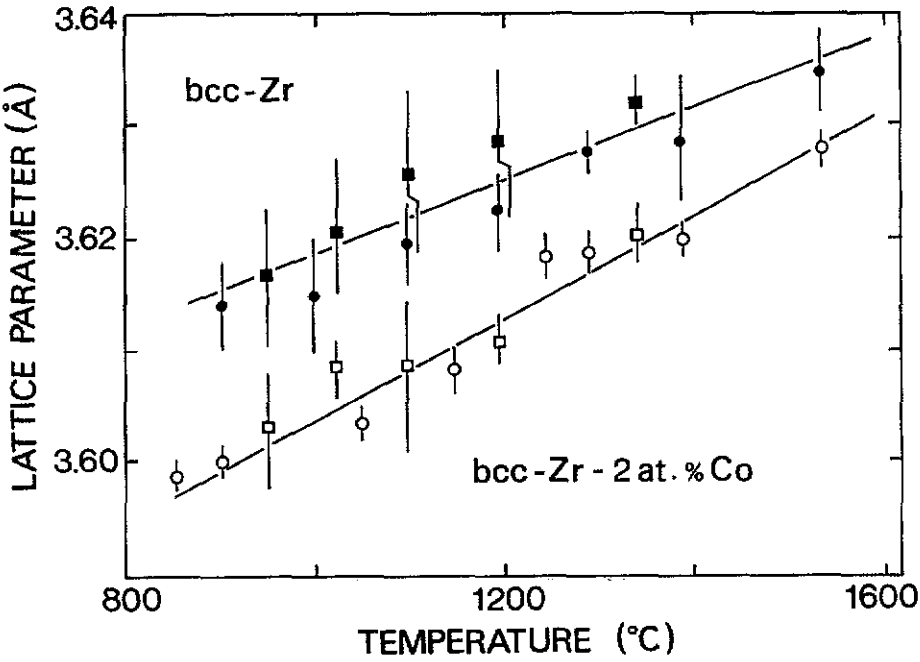

Figure 2. Lattice parameter of BCC Zr and BCC Zr–2 at.%Co: O, chipped samples; □, massive pellets. The large error bars for the results from the massive samples originate from uncontrolled recrystallization problems, which occasionally caused the disappearance of some of the Bragg peaks in the scattering plane.

Whereas all these arguments are strongly in favour of substitutional dissolved Co in BCC Zr, a minor fraction of Co on interstitial sites cannot be excluded. For instance, the stronger increase in the lattice parameter of Zr–2 at.%Co with increasing temperature, than for pure BCC Zr, might indicate that, with increasing temperature, an increasing fraction of Co is dissolved interstitially, thus causing a local expansion of the lattice.

Alternatively, the difference in temperature dependence of the lattice parameters could also be explained by an increase of anharmonicities in the interatomic potential in the alloy, in comparison to pure Zr.

4. Conclusion

The result of the present investigation has a major impact on models constructed so far for the fast solute diffusion of Co in BCC Zr. All models which are based on a major dissolution of Co in the interstitial sites can now be excluded [20]. The present results suggest that the majority of the Co migrates via vacancies similarly to Zr self-diffusion.

Such a model is in agreement with direct observations of the diffusion of Co or Fe in BCC Zr using microscopic methods such as quasi-elastic neutron scattering [2] or quasi-elastic Mössbauer spectroscopy [3]. In these experiments it is observed that the major fraction of the Co or Fe solutes diffuse approximately ten times faster than Zr self-diffusion, but this is still not fast enough to explain the net transport of mass as determined by tracer measurements [1, 4]. Based on this discrepancy it has to be

concluded that a minority fraction of Co or Fe atoms, which is not directly visible in the microscopic experiments, migrates very rapidly in order to explain the net transport of mass. Presumably such a very rapid diffusion occurs via interstitial sites. Whereas the quasi-elastic neutron studies on BCC Zr–2 at.%Co yield a maximum fraction of 28% of the Co atoms dissolved on interstitial sites, a recent study of Co induced lattice distortions in BCC Zr [7] and the present work give a strong indication of a considerably smaller fraction.

Finally we point out the similarities with the archetypal system of fast solute diffusion, i.e. the diffusion of Au in Pb. In this system a lattice contraction of the Pb matrix upon alloying with Au is also observed [21] and, by arguments similar to these presented here, it is concluded that the major fraction (> 80%) of Au dissolves substitutionally [21]. However, conclusions on identical diffusion mechanisms are limited by the considerable differences between the systems: Pb has a closed packed FCC structure, whereas BCC Zr exhibits an open lattice. The solubility of Au in Pb is extremely low of approximately 500 ppm at the melting point, whereas some 3 to 4 at.%Co or Fe can be dissolved in BCC Zr.

Acknowledgments

We thank G Vogl for his continuous interest and support. Financial support by the German Bundesministerium für Forschung und Technologie under the project numbers 03-ST1SPH-3 and 03-HE2MUE-0 is gratefully acknowledged.

References

[1] Kidson G V and Jung G J 1969 *Phil. Mag.* **20** 1047
[2] Petry W, Vogl G, Heidemann H and Steinmetz K H 1987 *Phil. Mag.* A **55** 187
[3] Yoshida Y, Miekeley W, Petry W, Stehr R, Steinmetz K H and Vogl G 1987 *Mater. Sci. Forum* **15–18** 487
[4] Trampenau J and Herzig C 1990 *J. Phys.: Condens. Matter* **2** 9345
[5] Heiming A 1989 *Thesis* Freie Universität, Berlin
[6] Heiming A, Petry W, Trampenau J, Alba M, Herzig Chr and Vogl G 1989 *Phys. Rev.* B **40** 11425
[7] Heiming A, Petry W, Vogl G, Trampenau J, Schober H R, Chevrier J, Schärpf O 1991 *Z. Phys.* B **85** 239
[8] Heiming A, Petry W, Trampenau J, Alba M, Herzig Chr, Schober H R and Vogl G 1991 *Phys. Rev.* B **43** 10948
[9] Skinner G B and Johnston H L 1953 *J. Chem. Phys.* **21** 1383
[10] Dorner B and Comes R 1977 *Topics in Current Physics* vol 3 (Berlin: Springer) p 127
[11] Lovesey S W 1984 *Theory of Neutron Scattering from Condensed Matter* vol 1 (Oxford: Clarendon)
[12] Sharp R I 1969 *J. Phys. C: Solid State Phys.* **2** 1969
[13] Petry W, Heiming A, Trampenau J, Alba M, Herzig C, Schober H R and Vogl G 1991 *Phys. Rev.* B **43** 10933
Trampenau J, Heiming A, Petry W, Alba M, Herzig C, Miekeley W and Schober H R 1991 *Phys. Rev.* B **43** 10963
[14] Warren B E 1969 *X-ray Diffraction* (New York: Addison-Wesley)
[15] Edwards J W, Speiser R and Johnston H L 1951 *J. Appl. Phys.* **22** 422
[16] Burgers W G 1934 *Physica* I 561
[17] Goldak J, Lloyd L T and Barrett C S 1966 *Phys. Rev.* **144** 478
[18] King H W 1966 *J. Mater. Sci.* **1** 79
[19] Eckerlin P, Kandler H 1971 *Landolt–Börnstein, Neue Serie* vol 6, ed K H Hellwege (Berlin: Springer)
[20] Hood G M 1975 *J. Phys. F: Met. Phys.* **6** 19
[21] Bolze T, Metzger H, Peisl J and Moss S C 1984 *J. Phys. F: Met. Phys.* **14** 1073, 1084